Proceedings World Geothermal Congress 2015
Melbourne, Australia, 19-25 April 2015

Reassessing Stimulation for EGS Reservoirs

Rob Jeffrey[1], Xi Zhang[1], and Reinhard Jung[2]

[1]CSIRO Energy, Private bag 10, Clayton South, Victoria, Australia 3168; [2]Jung Geothermal, Isernhagen, Germany

[1]rob.jeffrey@csiro.au, xi.zhang@csiro.au, [2]jung.geotherm@gmail.com

Keywords: EGS Stimulation, geothermal, hydraulic fracture, wing fracture

ABSTRACT

Although the original attempts to stimulate hot dry rock or enhanced geothermal system (EGS) reservoirs employed conventional hydraulic fracturing methods, initial difficulty in obtaining sufficient connection between the stimulated zone and a targeted production well was experienced. Furthermore, the measurement of a cloud of microseismicity associated with the injections suggested shearing of natural fractures as an important process and led to development of stimulation methods that rely on shear-induced dilation to create reservoir permeability. Since this early change in approach, the process of stimulation applied to EGS reservoirs has continued to be founded on promoting shearing of natural fractures in the rock mass by injection of large volumes of water into long open-hole sections of the well at rates that limit the pressure to be at or below the fracture opening pressure.

Shearing of natural fractures with the formation of wing fractures that then link between otherwise unconnected natural fractures provides a mechanism for development of directional conductive pathways when stimulation is carried out at or below fracture opening pressure. In particular, placing multiple fractures along a wellbore completed using a cemented casing string is expected to produce a better stimulation result compared to injection into a long openhole section. In addition, analysis of opening mode hydraulic fractures placed into hard, naturally fractured rock using pressures well above the minimum principal stress magnitude and then mapped in mineback experiments, show these fractures grew in the direction perpendicular to the minimum principal stress with offsets in their path developing at sites where the opening mode fracture interacts with and crosses natural fractures. This provides another mode of fracture growth that could be used to stimulate EGS reservoirs, provided cemented casing strings are used to complete the well.

1. INTRODUCTION

The concept of extracting geothermal heat by connecting two wells using hydraulic fractures was proposed for the first well pairs drilled at the Fenton Hill site in New Mexico, operated by Los Alamos National Laboratory. At that point in time, as described by Jung (2013), hot dry rock reservoir development was proposed to be carried out by placing one or more hydraulic fractures into the reservoir to act as the main connection between wells and to provide the heat exchange surface area. The first hydraulic fracturing at Fenton Hill produced two vertical closely spaced fractures, striking N35E (Smith et al., 1975). Further injections generated an associated cloud of microseismic activity and this observation led to the recognition that shearing on natural fractures was an important process that might be exploited so that a volume of rock could be stimulated by shear-induced dilation alone. Thus, two different approaches, illustrated in Figure 1, to generate geothermal reservoir conductivity and surface area were proposed with the method relying on shearing and dilation of natural fracture selected as the preferred option.

In order to promote shearing, wells were completed with openhole sections and injections were carried out into these sections without zonal isolation at rates controlled to maintain the bottomhole injection pressure below the magnitude of the minimum principal stress, which avoided the formation of opening mode hydraulic fractures. Sliding on natural fractures in the rock mass is promoted by raising the fluid pressure in these fractures, reducing the effective normal stress so that the in situ shear stress acting on them exceeds their reduced shear strength. The conductivity of the natural fracture is enhanced at the same time by shear-induced dilation which results from roughness and asperities of the fracture faces riding up on one another as shearing occurs (Lockner and Byerlee, 1994). This process has been applied to every geothermal EGS reservoir since the work at Fenton Hill. The stimulation achieved has been significant, but not sufficient to enable commercial circulation rates to be carried out. Because the injection is carried out into large openhole sections of the wellbore, the fluid finds the easiest pathway and commonly only one or two zones take most of the fluid. The lack of any method for isolating zones in this openhole section also means that it is not possible to control the injection to better stimulate zones between the naturally conductive sections.

Therefore, in this paper we consider two alternative methods of stimulation for application to EGS reservoirs. One of these methods is a return to the first concepts proposed for reservoir stimulation at Fenton Hill by stimulating and connecting two or more wells using a series of hydraulic fractures placed from a cased and cemented wellbore. The second method also requires a cased wellbore but relies on enhancing the natural fracture conductivity and connecting these together by taking advantage of wing fracture growth. Growth of fractures by both mechanisms is analyzed numerically using a fully coupled hydraulic fracturing model. Depending on the stress regime present in the reservoir, horizontal wells may be required to allow multistage fracturing. Alternatively, vertical wells can be used to place multiple horizontal fractures if the minimum stress is vertical. In either case, the wells must be completed with a cemented casing string across the target interval. With these changes, wells can be stimulated to effectively connect injection and production wells with 10 or more conductive discrete zones. Such an approach will allow for more complete engineering of the EGS reservoir to produce a conductivity that allows commercial circulation rates to be achieved.

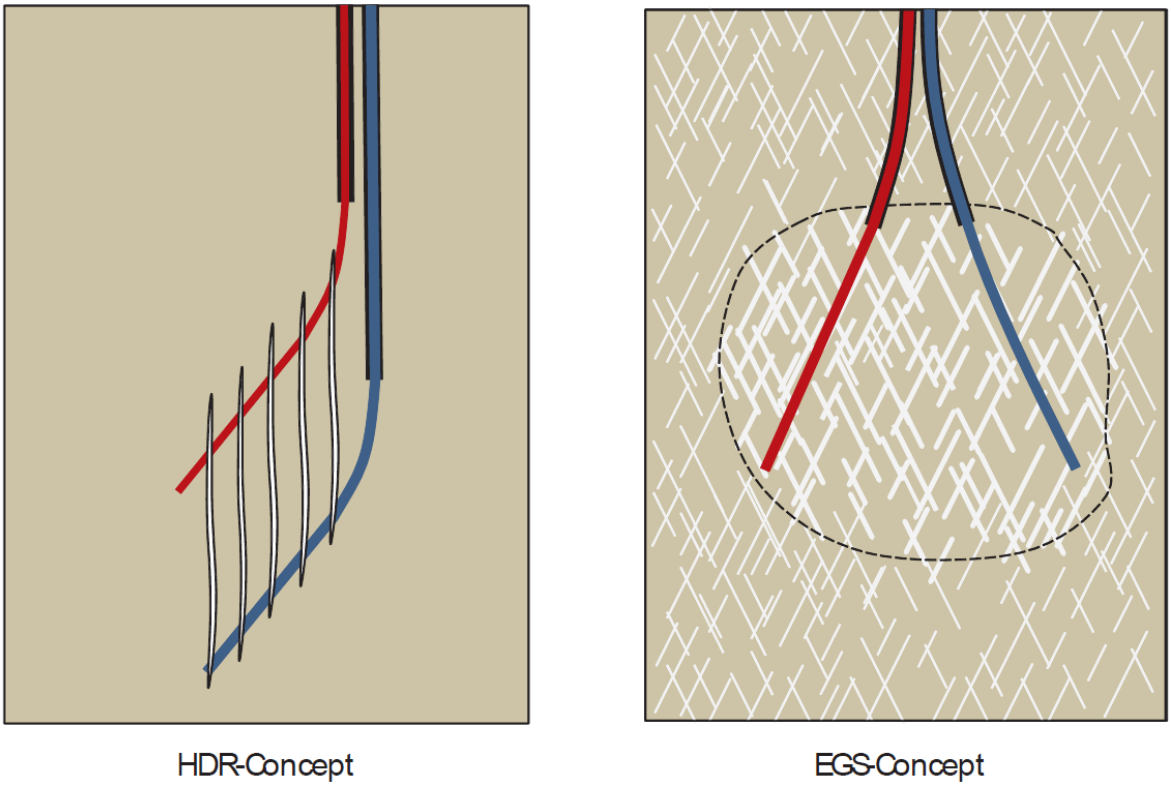

Figure 1: The two concepts for stimulation of geothermal reservoirs (from Jung, 2013).

2. SHEAR AND OPENING MODE FRACTURE GROWTH

Hydraulic fractures grow in the direction that requires the least amount of energy. In an unfractured rock mass, this direction is perpendicular to the minimum principal stress direction. In fractured rock, the hydraulic fracture may be guided locally by a natural fracture in a direction that is not perpendicular to the minimum stress, but the hydraulic fracture will escape the natural fracture when it encounters a flaw or when it reaches the tip of the natural fracture (Zhang et al., 2006). The entry and exit from the natural fracture leaves an offset in the fracture path, which vary in size from millimeters to several meters. Fractures with offsets have been mapped in several mineback experiments (Warpinski and Teufel, 1987; Jeffrey et al., 2009a), and are found in laboratory experiments (Daneshy, 1974; Daneshy, 2003) and their effect on fracture growth has been analyzed numerically (Jeffrey et al., 2009b; Zhang et al., 2006; Zhang and Jeffrey, 2008; Weng et al., 2011). The overall fracture geometry consists of sections aligned perpendicular to the minimum principal stress direction with offsets occurring as the fracture interacts with and crosses natural fractures.

In contrast to hydraulic fracturing, shear fracturing occurs on the natural fractures in response to a reduction of the effective normal stress as the fluid pressure in the fracture is increased. The fluid pressure is always less than the normal stress magnitude as otherwise opening of the natural fracture occurs. The goal of inducing shear on the natural fractures is to enhance their hydraulic conductivity by shear-induced dilation of the fractures. The rough and wavy surfaces of the natural fracture ride up on one another during the shear process, leaving behind a more conductive fracture. This stimulation process occurs at injection pressures below the minimum principal stress magnitude and is enhanced by use of a low viscosity fluid which can more easily enter and pressurize the natural fractures to produce the stimulation by shearing. The microseismicity recorded during injection into geothermal reservoirs is an expression of shearing occurring with unstable slip generating the seismic events. Microseismicity is also associated with hydraulic fracturing as fluid is lost from the main fracture channel into cross-cutting natural fractures. Shear fracturing is often envisioned as being accompanied by extension of the natural fracture in its own plane, but it is equally common for so called wing fractures to be generated near the tips of the natural fracture. These wing fractures are extended by the shear deformation of the main fracture and curve to align themselves with the maximum stress direction. Even without considering shear-induced dilation, the deformation associated with wing fracture growth produces opening of the wing fracture which is maximum at the root of the wing fracture with potential for pipe-like conduits forming along these junctions.

2.2 Wing Fracture Growth

Wing fractures form at or near the tip of a fracture subject to shearing as a result of the tensile stress induced in these near-tip regions (e.g., Cooke, 1997). A natural fracture undergoing shear could have a variety of shapes. An elliptical fracture (flaw) that has been subject to shear with resulting wing crack growth is shown in Figure 2. The sample of transparent material was loaded uniaxially in this case with a compressive load applied across the vertical direction. The wing fractures form along the arc of the leading edge of the flaw and reorient to align with the applied compressive stress, but they retain a considerable amount of curvature (Dyskin et al., 1999). When a second stress is applied to the sample so that a condition of biaxial compression exists, the wing fracture growth becomes more planar, making further extension of the wing fractures to great lengths possible (Sahouryeh et

al., 2002). In this paper the 3D problem is considered in 2D by taking a section through the center of the wing crack. This simplifies the geometry considerably, but the complexity of solving the coupled fluid pressure, fracture opening and fracture shearing remains.

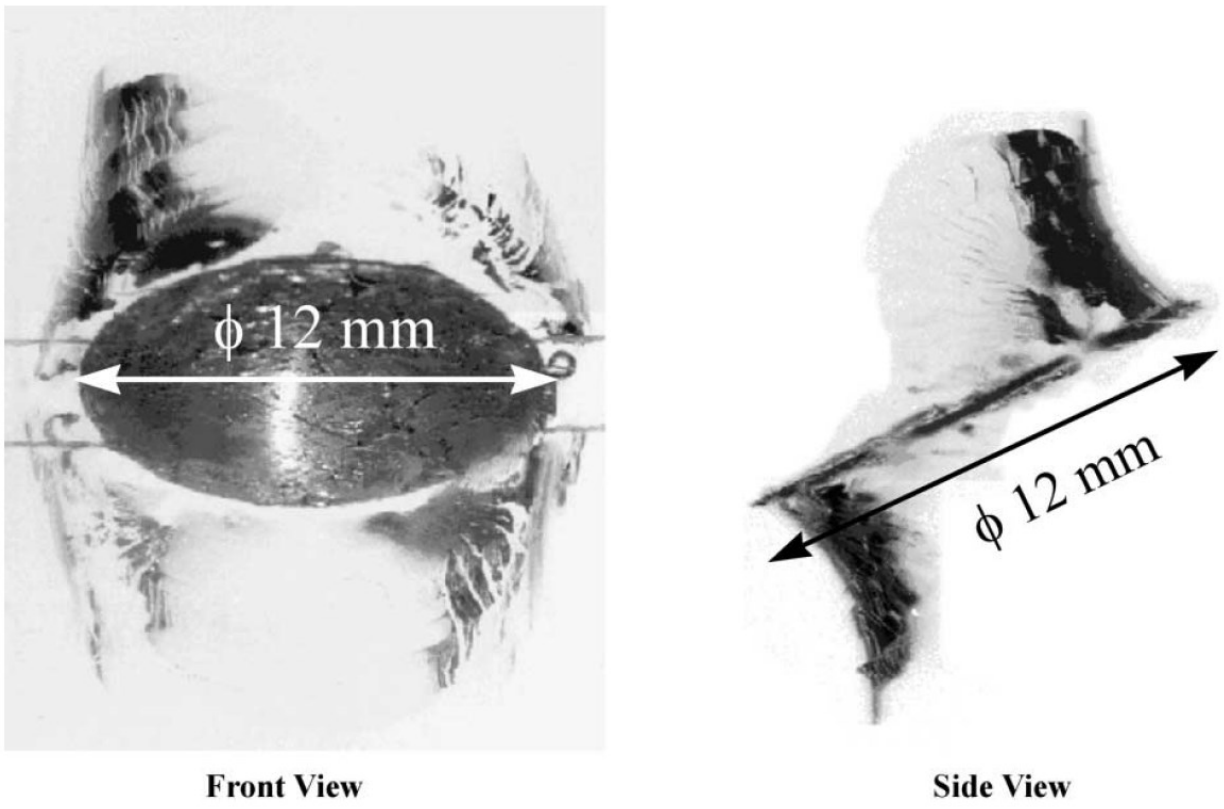

Figure 2: 3D wing fracture in transparent resin (From Sahouryeh et al., 2002).

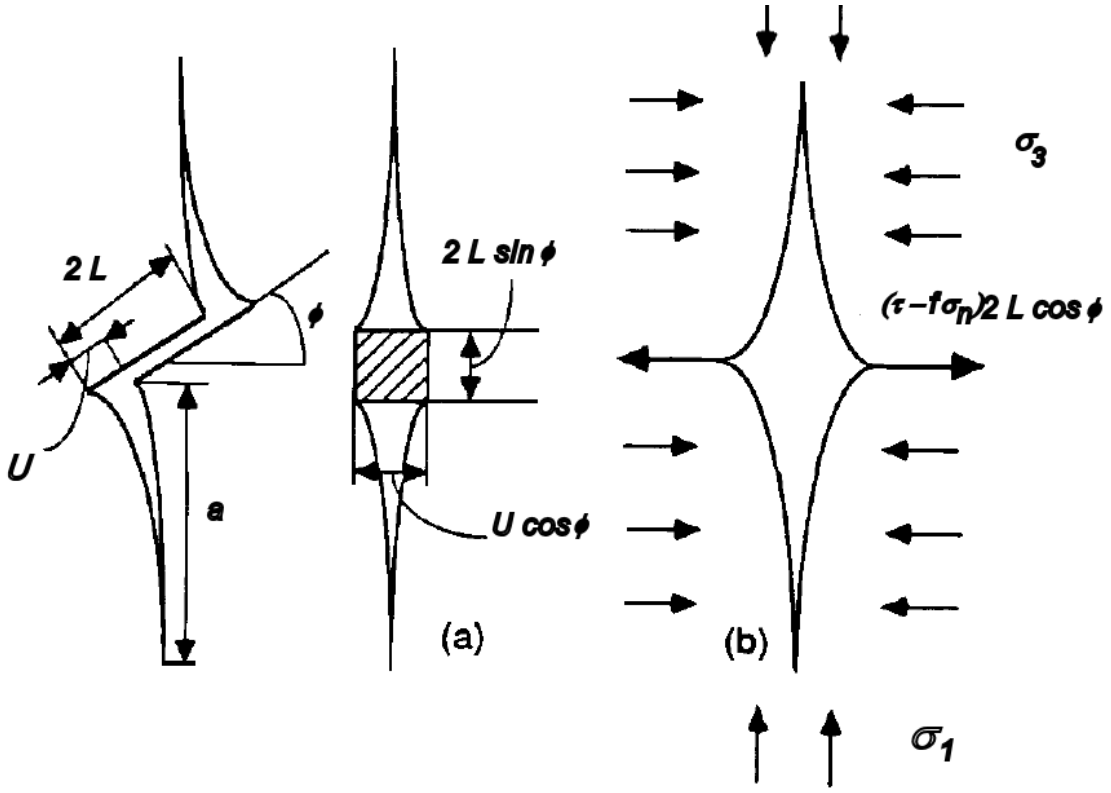

Figure 3: Simplified analysis of a 2D wing crack subject to uniaxial compression (after Lehner and Kachanov (1996).

The fracture mechanics of wing fracture growth under bi-axial compression can be illustrated by considering the 2D problem shown in Figure 3, which is modified from Lehner and Kachanov (1996) and Dyskin et al. (1999), and the analysis given here is in line with that originally given by Fairhurst and Cook (1966). The wing cracks extend as a result of sliding on the initial flaw of length 2*L* oriented at an angle ϕ with respect to the applied minimum principal stress σ_3. As the flaw is assumed to be in frictional sliding, its shear force, contributing to slip, is given as $(\tau - f\sigma_n^N)2L$, where σ_n^N is the effective normal stress across the natural fracture and *f* is the coefficient of friction of the natural fracture. Furthermore, the resultant horizontal force, which contributes to the opening mode stress intensity factor of the wing fractures, is found to be given by

$$F = (\tau - f\sigma_n^N)2L\cos\phi \qquad 1$$

Knowing F, the stress intensity factor for the simplified problem of Figure 3b is given by (Tada et al., 1985)

$$K_I = \frac{F}{\sqrt{\pi l}} \qquad 2$$

where *l* is the effective half length of the main-wing fracture system. And the wing fracture length at which $K_I = K_{Ic}$ can be found for any *F* value.

Axial splitting of rock subject to uniaxial loading is often attributed to linking up of a number of wing fractures growing from flaws and driven by this mechanism. In a geothermal reservoir, the natural fractures are subject to a 3D stress field and the wing fractures can be expected to grow with some non-planar geometry. As already discussed, the driving force arises from the reduction in the effective normal stress acting across the natural fracture because of injection induced fluid pressure increases, resulting in a weakening of the shear strength of the natural fracture, which allows the far-field shear stress to induce sliding on the fracture, resulting in wing fracture formation and growth.

2.3 Opening Hydraulic Fracture Growth

The opening mode hydraulic fracture growth problem is also simplified by treating it as a 2D problem. From this analysis, some of the main features of hydraulic fracture growth in a naturally fractured rock mass are highlighted. The same 2D numerical model is used for this analysis as is used for the shear and wing fracture growth analysis, but the injection rate and fluid viscosity used are such that the growing fracture is opened hydraulically rather than undergoing only shearing and sliding. Some shear deformation occurs in the opening mode hydraulic fracture and some opening occurs in the shearing wing fracture system because of the non-planar fracture geometries generated by both processes in a naturally fractured rock. The hydraulic fractures are grown using an injection pressure that is higher than the minimum principal stress magnitude and the wing fractures are grown using an injection pressure that is always less than the minimum stress.

3 WING FRACTURE STIMULATION

For wing fracture growth driven by injection of fluid, the effect of the fluid pressure needs to be included in an equation predicting growth of the wing fractures.

3.1 Comparison of Analytical and Numerical Results

In this section, we compare results from a simplified analytical solution for wing fracture growth (Kachanov, 1982 and Lehner and Kachanov, 1996) to results from the 2D numerical model. Kachanov (1982) modified the opening-mode stress intensity factor given by Cotterell and Rice (1980) by adding an additional term associated with a moderately small wing crack size,

$$K_I = \frac{2}{\sqrt{3}}(\tau - f\sigma_n^N)\sqrt{\pi L} - \sigma_n^W\sqrt{\pi a} \qquad 3$$

where $\sigma_n^W = \sigma_3$ (see Figure 3) is the effective normal stress across the wing fracture portion.

This equation was further modified by Lehner and Kachanov (1996) by considering that the value of *l* is represented by the sum of the wing fracture length and a "nucleus" length associated with the natural fracture, that is $l = a + \kappa L$ with $\kappa = 3\cos^2\phi/\pi^2$. Lehner and Kachanov (1996) thus obtained a formula that converges to the correct solution for both a short and long wing crack. The opening mode stress intensity factor for the wing crack system is given by them as

$$K_I = \frac{(\tau - f\sigma_n^N)2L\cos\phi}{\sqrt{\pi(a + 3L\cos^2\phi/\pi^2)}} - \sigma_n^W\sqrt{\pi a} \qquad 4$$

If *a* is much smaller than *L*, this equation reduces to Eq. 3, the result of Kachanov (1982).

Appling the toughness criterion for fracture growth, the above equation can be written as:

$$\frac{K_{Ic}}{\sqrt{L}} = \frac{(\tau - f\sigma_n^N)2\cos\phi}{\sqrt{\pi(a/L + 3\cos^2\phi/\pi^2)}} - \sigma_n^W\sqrt{\pi a/L} \qquad 5$$

We note that the normal stresses are effective stresses and depend on the fluid pressure. It is assumed that the fluid pressure is uniform in the fracture. By solving the above non-linear equation, we can obtain the relation between *a/L* and the fluid pressure.

Figure 4 contains a graph showing how the predicted value of *a/L* varies with injection pressure according to Eq. 5 and as calculated by the numerical model when using the simplifications used in deriving Eq. 5. The third and fourth curves are obtained from the numerical model for cases where the wing fracture is allowed to curve as it extends from a natural fracture that is included in the model so the fracture geometry is similar to the 2D problem shown at the left side of Figure 3. The analytical and numerical solutions agree well with each other (Figure 4) for the simplified problem used in deriving Eq. 5. The blue and black curves then show the effect of including a more realist wing fracture geometry so that the wing fractures curve as they grow to align with the maximum stress direction.

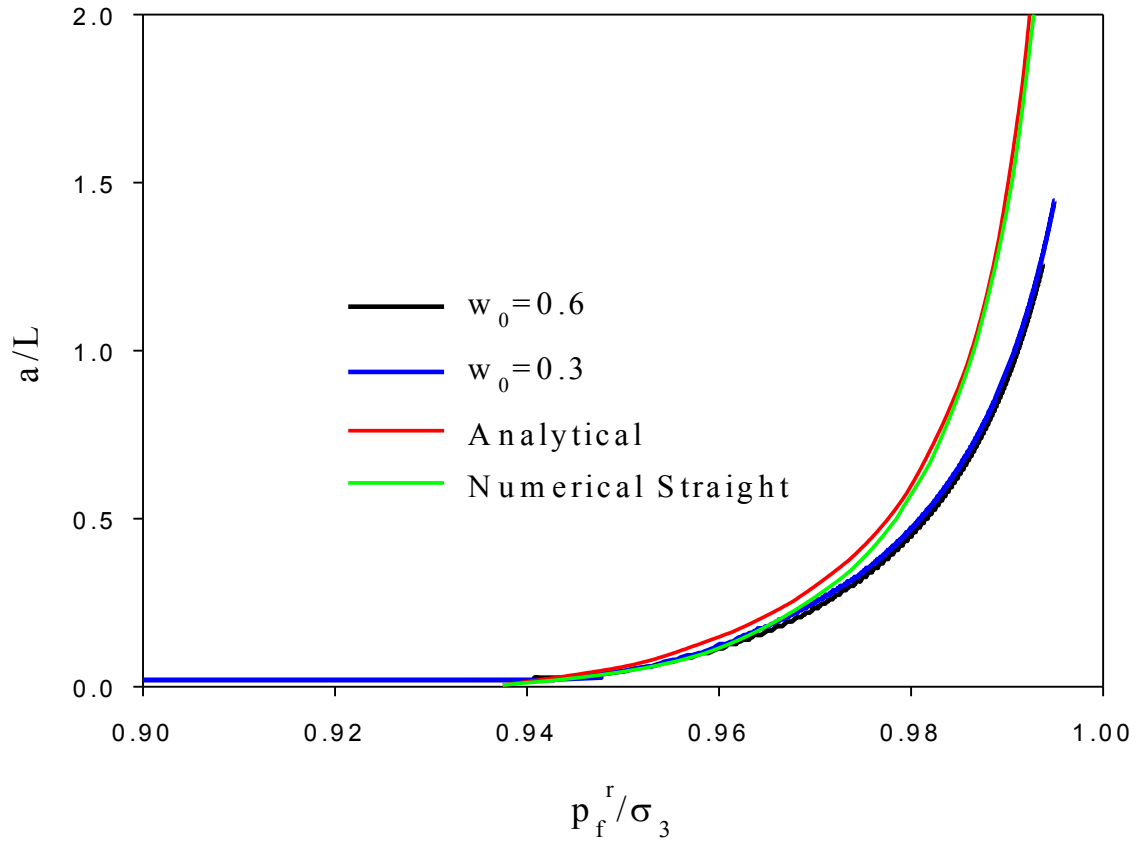

Figure 4: Variations of wing fracture length, *a*, with the dimensionless pressure measured at the root of the wing fracture, for the case where σ_3 =83.2 MPa. For these conditions, slip on the natural fracture starts at the injection point when p_f^0/σ_3 =0.931 (p_f^0 is the injection pressure). And the wing fracture starts to grow when p_f^r/σ_3 =0.933, immediately after the onset of slip. The time period associated with this small pressure increase, but rapid slip development, is very short, which results in some numerical instability if the time step is not small enough.

As a limit, when the fluid pressure is equal to the compressive normal stress across the wing, we get the maximum wing fracture length for a case where the wing fracture is not opened hydraulically, based on Eq. 5. For the parameters used to construct the curves in Figure 4 this *a/L* value is 250 and, if the pressure is increased slightly above the magnitude of σ_3 , the wing fracture growth is unstable. However, injection at rates sufficient to open the wing fractures will result in non-uniform pressure inside the natural fracture and the wing fractures, as fluid viscous friction becomes important. A numerical hydraulic fracture model must then be used to solve for the pressure distribution and the wing fracture opening and growth.

3.2 Numerical Analysis for Wing-Crack Growth Connecting Natural Fractures

The basis of the process of stimulation of a reservoir by wing fracture growth relies on the wing fractures growing to sufficient length that they connect into adjacent, otherwise unconnected, natural fractures. A number of natural fractures can then be linked up into a conductive network, providing the flow path for fluid circulation through the reservoir. Wing crack growth is considered

using the simplified two-dimension fracture problem, which can be considered as a section through a 3D fracture, cutting the 3D fracture along the central line. The parameters, which are kept unchanged throughout the paper, based on parameters typical of an EGS reservoir (Jung, 2013), are listed in Table 1. The fluid injection rate is given as used by the 2D model in terms of per meter of fracture thickness (out of the 2D plane).

Table 1: Parameters held constant during numerical analysis

Parameter	Value
Rock Young's modulus (E)	50 GPa
Poisson's ratio	0.22
Rock Fracture Toughness	1.0 MPa $\sqrt{m}$
Fluid dynamic viscosity	0.0005 Pa.s
Fluid Injection Rate	$2x10^{-4}$ m^2/s
Coefficient of friction of natural fracture	0.8

Among the several hundreds of natural fractures intersected by the wellbore and present in the very long openhole sections of an EGS-well, there will always be a few with initial fracture transmissivities or conductivities of at least 10^{-14} m^3. This transmissivity corresponds with an aperture of 0.05 mm. If we allow for some enhancement of this transmissivity caused by shear-induced dilation, the initial aperture used in the numerical cases presented below is assumed to be larger than 0.05 mm.

Several different 2D stress conditions (cases) are used in the analysis and are given in Table 2.

Table 2: Stress conditions considered in the numerical analysis of wing fracture growth

Case	σ_{xx} (MPa)	σ_{yy} (MPa)	σ_{xy} (MPa)	σ_1 (MPa)	σ_3 (MPa)	σ_3/σ_1 (MPa)	θ (degrees)
a	98	90	-10	104.8	83.2	0.794	34.1
b	98	70	-10	101.2	66.8	0.660	17.8
c	98	60	-10	100.5	57.5	0.572	13.9

Notes: (1) Compressive stress is positive.

(2) Shear stress is positive if the stress direction vector times the unit normal vector to the surface the stress acts on is positive.

(3) The principal stress angle is with respect to σ_{xx}.

Three initial fracture geometries were used in the numerical analysis and are shown in Figure 5. The main natural fracture is oriented at an angle to the principal stress according to the values given in Table 2. For each case, injection of fluid is simulated so that the effective normal stress acting across the natural fracture is progressively reduced, causing shear sliding to occur on the natural fracture and resulting in wing fracture growth.

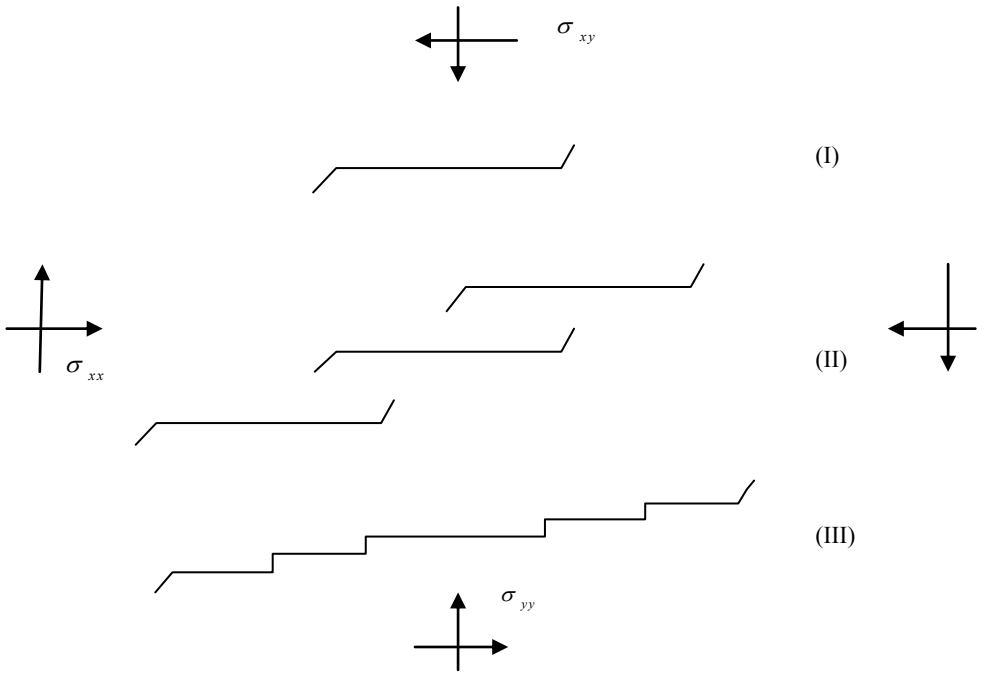

Figure 5: Initial fracture geometries considered. The wing fracture starts from the tip of the natural fracture. Three cases are considered, ranging from one fracture to five that link up via wing fractures.

The numerical model and assumptions

Fracture propagation is based on the stress intensity factor equaling the fracture toughness with the propagation direction found based on the criterion proposed by Erdogan and Sih (1963). The fracture trajectory found by the numerical model can be a curved path, instead of a straight line as was assumed in the analysis of Lehner and Kachanov (1996). A damping factor (0.2 used here) is used together with a restriction that the opening mode stress intensity factor is always non-zero to limit the tendency for fracture zigzagging to occur. The wing fracture growth starts from a small initial fracture located at the tip of the natural fracture oriented at an angle of 70 degrees to the natural fracture direction. This small starter fracture is given a length equal to three percent of the natural fracture half-length. Both the natural fracture and the wing fracture can undergo shear and opening deformation. The shear strength of the fractures is assumed to follow a Coulomb friction law without shear induced dilation or cohesion.

The numerical model has been verified by comparison to analytical fracture mechanics results (see Zhang et al., 2007) and analytical hydraulic fracture mechanics results (see Detournay, 2004). In the analysis presented here, the possibility of fracture initiation at a flaw located along the natural fracture, some distance from the tip, is not considered. Only one wing fracture pair is allowed to initiate and these always are located at the tips of the natural fracture. Cooke (1997) and Multu and Pollard (2008) provide cases where more than one wing fracture initiates from the natural fracture.

If the pre-existing nature fracture is of low enough hydraulic conductivity, the injection causes the fluid pressure to become larger than the normal stress acting across the natural fracture and the fracture is opened hydraulically. Therefore, the initial magnitude of the fracture aperture is an important parameter if the fluid pressure is to be kept below the minimum stress level. Using a lower injection rate and / or a lower fluid viscosity will also allow injection to be carried out at a pressure below the opening pressure, but there is a lower limit on the viscosity and, in practice, the injection rate must be sufficiently high to inject a fairly large volume of fluid in relatively short time (days to weeks) because of cost considerations. For this reason, most EGS stimulations that are designed to promote shearing in the rock mass end up injecting at pressures approaching the magnitude of the minimum principal stress.

Effect of minimum principal stress and orientation of natural fracture

The results of the numerical modeling indicate that wing fracture propagation only occurs to a significant length when the fluid pressure is near the minimum principal stress in magnitude (see Figure 6). Figures 6 and 7 shows several results that illustrate this behavior. As the wing fractures extend, they become oriented to align parallel to the maximum principal stress direction and open against the minimum principal stress. Figure 8 shows opening and shear displacement along the natural fracture and the wing fracture. The wing fractures are opened except very near the tip. Large shear displacements occur along the natural fracture and these generate large opening of the wing fractures roots, where they initiated from the natural fracture. This shear slip transfer acts as a driving force for wing fracture growth, as illustrated in Figure 1. The opening is aided by the fluid pressure which reduces the effective normal stress acting on the wing fracture to a low value. Initially, when the wing fracture is short, the opening induced by shearing of the natural fracture has a stronger effect, allowing this shorter wing fracture to extend even when the fluid pressure is lower. As the wing fracture extends, the opening at its root becomes less and less effective in extending it further and the fluid

pressure increases to compensate. Eventually, for a given set of parameters and for a long enough wing fracture, the pressure must increase until it exceeds the minimum stress magnitude or otherwise the wing fracture will arrest.

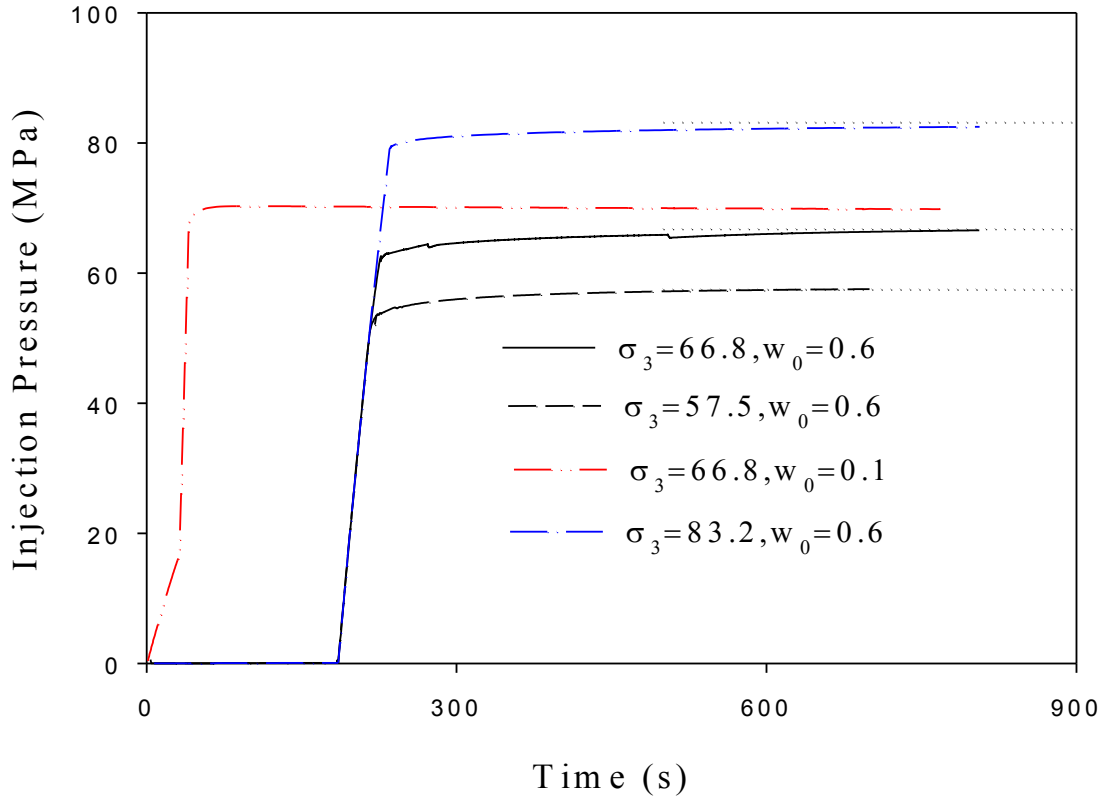

Figure 6: Variation of injection pressure with time for different minimum principal stresses and natural fracture apertures. The minimum stress magnitude is shown by a dotted line for each case. Note the red line corresponds to opening mode hydraulic fracture growth.

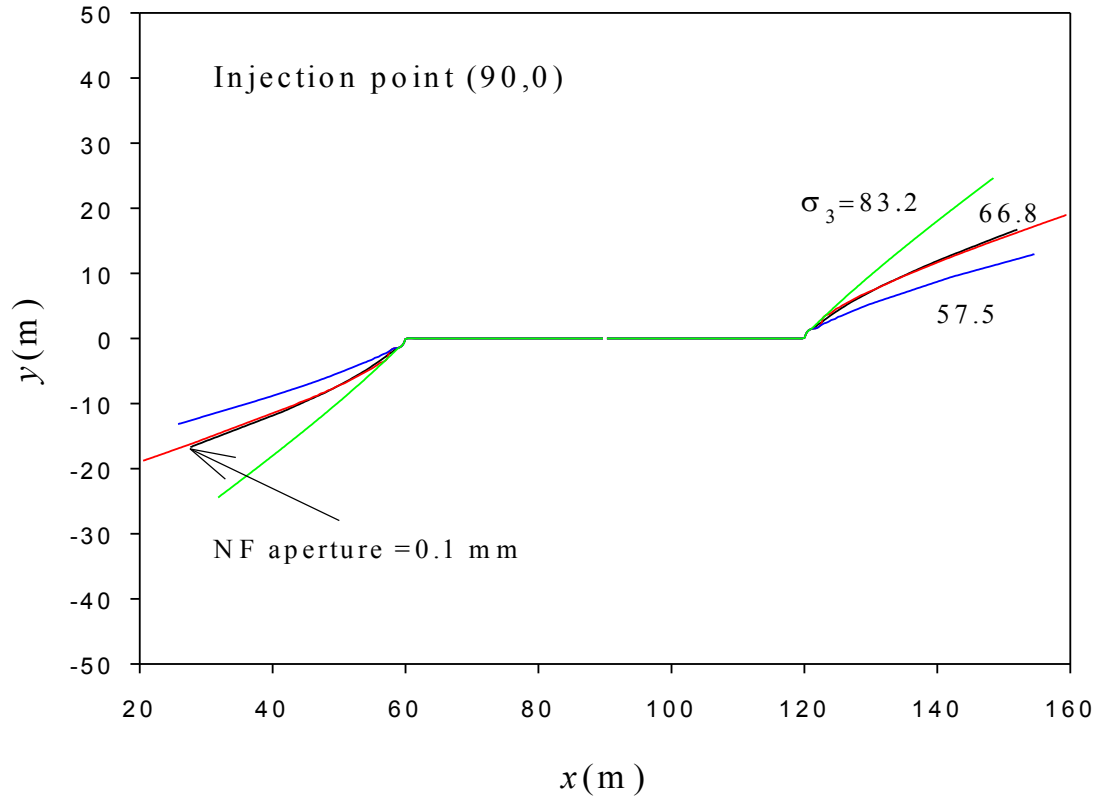

Figure 7: Fracture trajectories for different minimum principal stress and natural fracture apertures (see Table 2 for stress conditions used). The scales used for the two coordinates are equal. Pressure history is shown in Figure 6.

In Figure 8, a case is shown where a very large shear displacement has developed along the natural fracture and a large induced opening exists at the root of the wing. However, although the opening along the natural fracture is still small, there is a region of opening on the natural fracture near the wing fracture root. This is in contrast to the assumption used by Nemat-Nasser and Horii (1982) where no such opening was allowed.

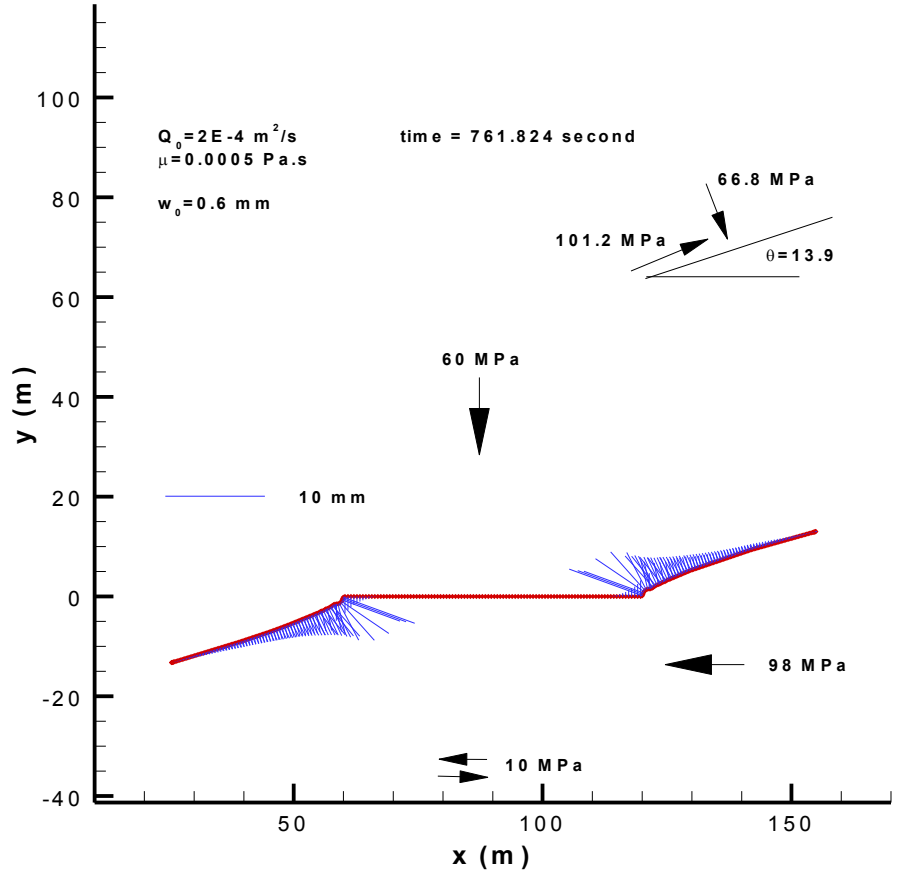

(a) opening

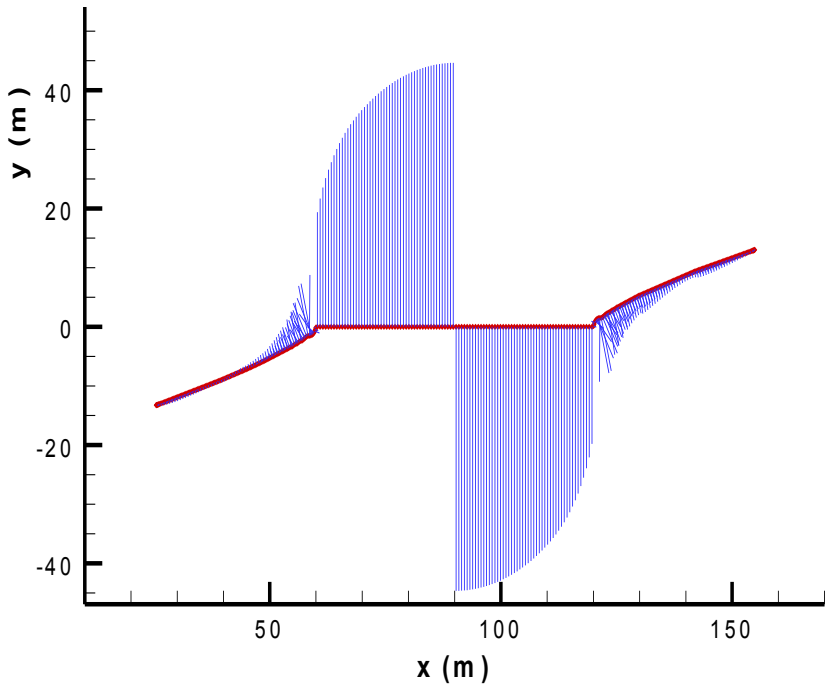

(b) shearing (with the same scale)

Figure 8: The opening (a) and shear (b) displacements along the natural fracture and the wing fractures are given by the lengths of the bars drawn normal to the fracture surface.

Connected system of natural fractures with wing fractures

The connection of a wing fracture with other natural fractures must be considered if wing fracture growth is to play a role in forming the main conduit for injected fluid during circulation. One special case to be considered is how the wing fractures grow from an already connected fracture system undergoing shear where the connected fractures form a chain of natural fractures and of wing fractures which link the natural fractures. How this system of fractures responds to further shearing and whether larger wing fractures will form at the ends of this system is an open question (Jung, 2013). The case modelled is shown in Figure 9, where the starting geometry consists of the natural fractures and the connecting 1 m long segments (representing wing fractures formed earlier). Four of these connections were meshed to generate the initial geometry and these divide the shear zone into five horizontal segments, which are specified to be very permeable. The injection pressure at the time shown is 65.64 MPa. It is seen in Figure 9 that the wing fractures, even though subjected to a larger compressive stress, are widely opened. This is attributed to the intensive slip along the horizontal segments. Because of their opening width, a large volume of fluid is stored in these segments even though they are relatively short and the fluid volume needed to fill and open these segments slows further wing fracture initiation.

With continued injection the wing fracture growth becomes non-symmetry, as shown in Figure 9(b). Small changes in the conductivity between the injection point and the tip of the fracture system lead to higher conductivity on one side and this leads to more wing fracture growth on that side. No perturbation was imposed in the calculation, but rather the asymmetry arose from the small numerically generated differences between the fracture sides. Width restrictions occur along the wing fracture where it turns and reorients. This makes the numerical results more sensitivity to small perturbations. These effects need further investigation.

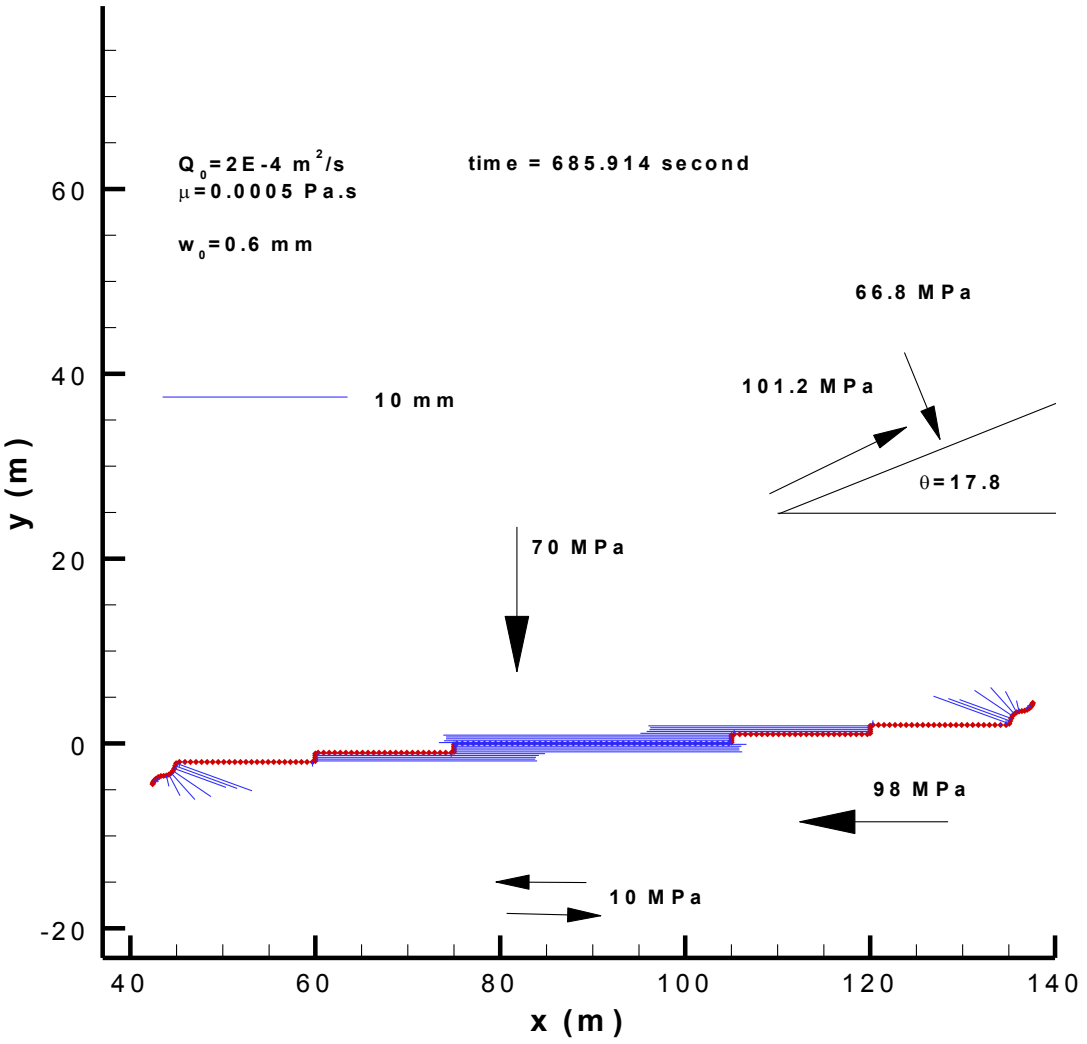

(a)

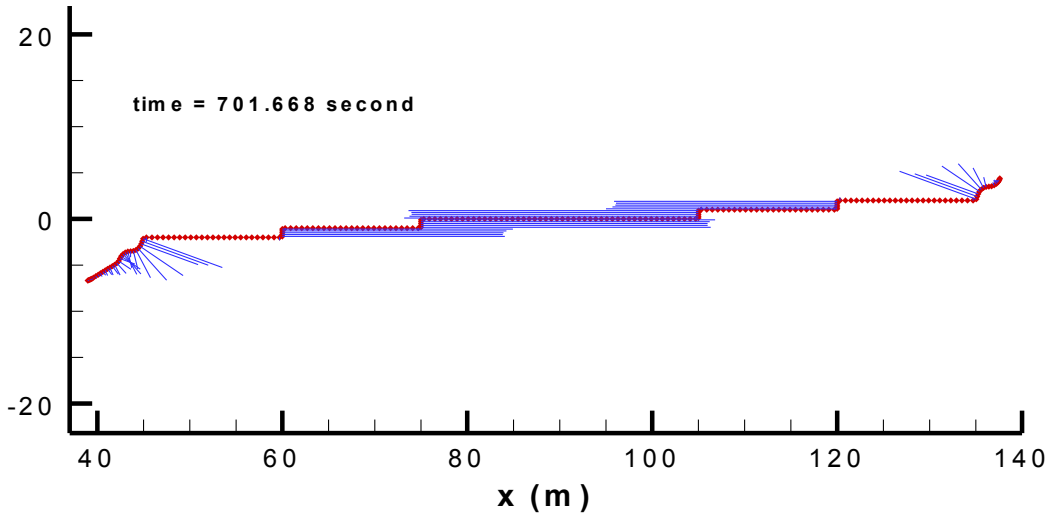

(b)

Figure 9: Opening along the offset fracture chain at two time instants. The injection point is at (90,0).

Intersection details

Another important situation related to the wing fracture connection is how a wing fracture connects to another natural fracture and how a new wing fracture is nucleated from this natural fracture. In Figure 10, the injection point is located at (90,0) in the center of the middle natural fracture. The geometry for the other two natural fractures is shown in Figure 10. As a result of the injection of fluid into the center fracture, two wing fractures have developed from the ends of the middle natural fracture and propagated towards and into the other two natural fractures.

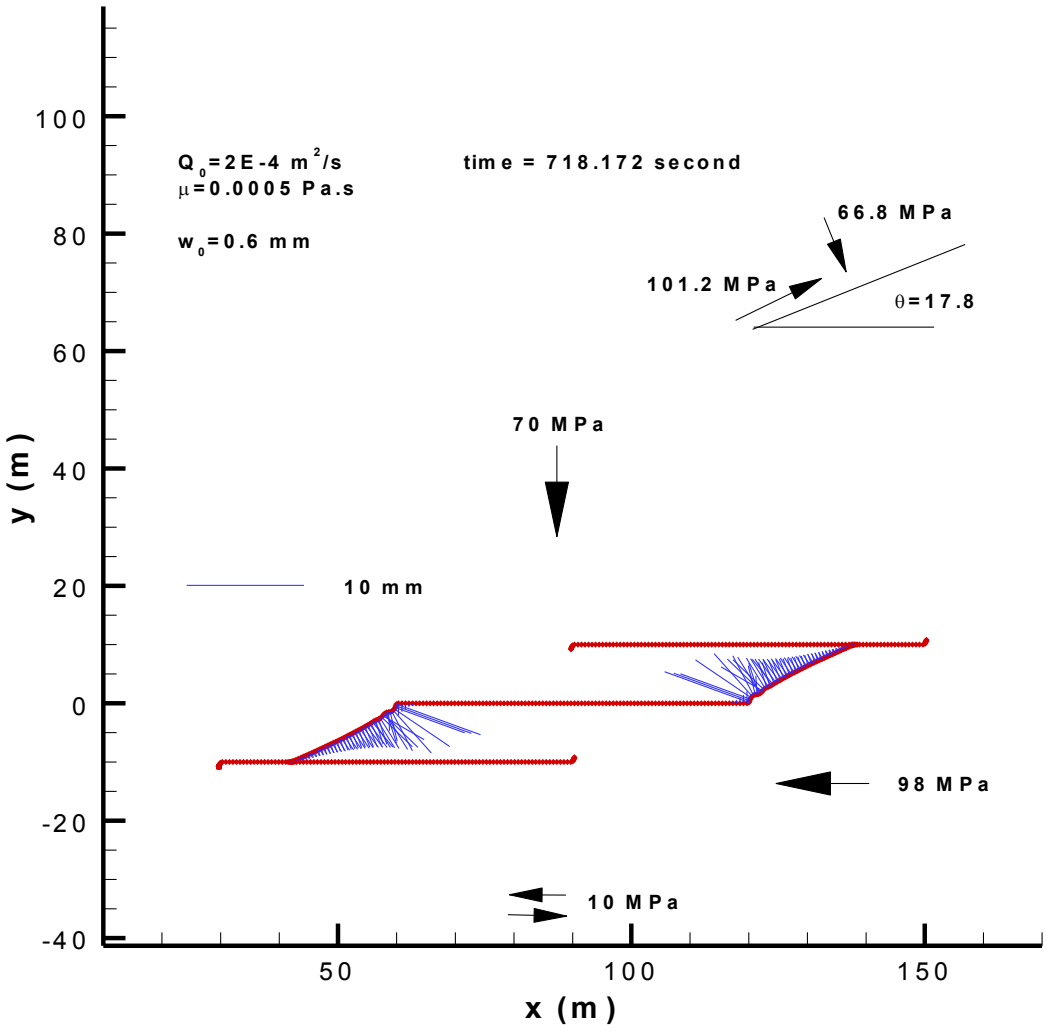

(a) opening

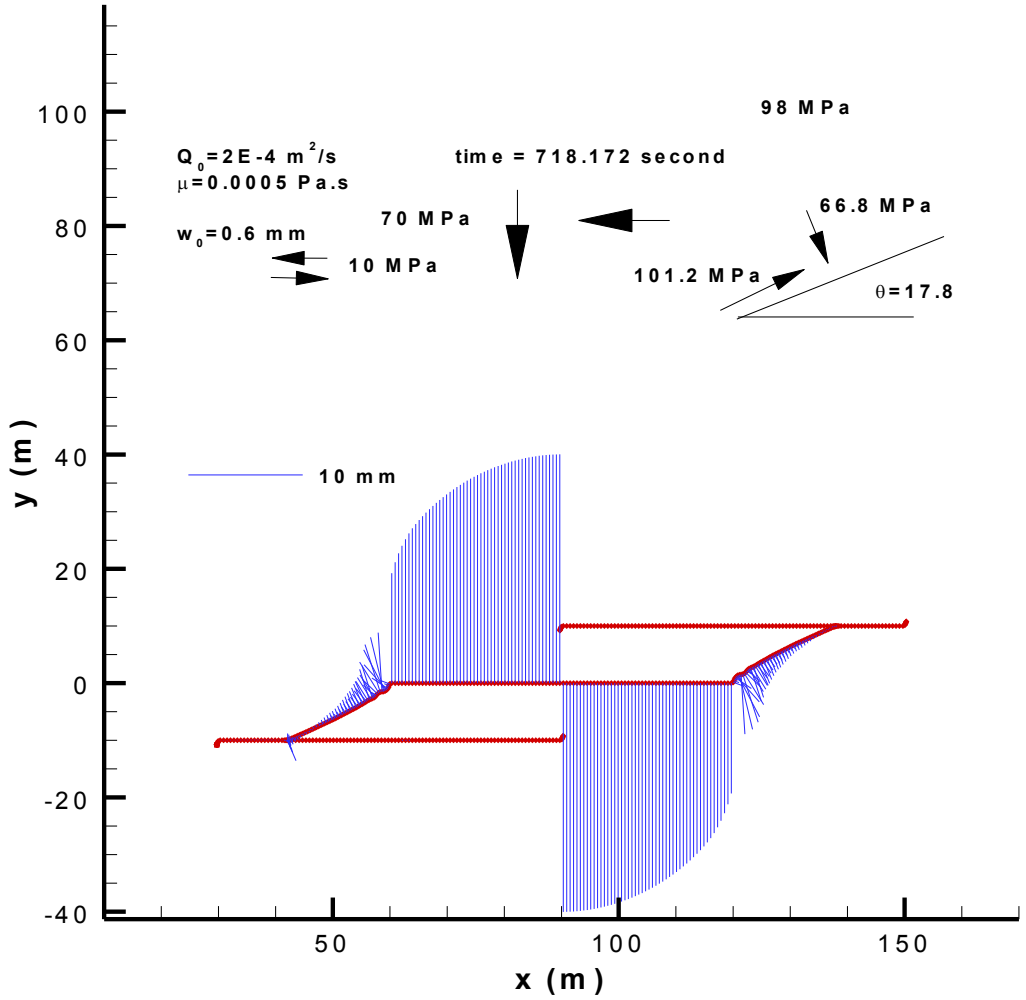
98 MPa
Q0=2E-4 m2/s
μ=0.0005 Pa.s
time = 718.172 second
w0=0.6 mm
70 MPa
66.8 MPa
10 MPa
101.2 MPa
θ=17.8
10 mm
y (m)
x (m)
100
80
60
40
20
0
-20
-40
50
100
150

(b) shearing

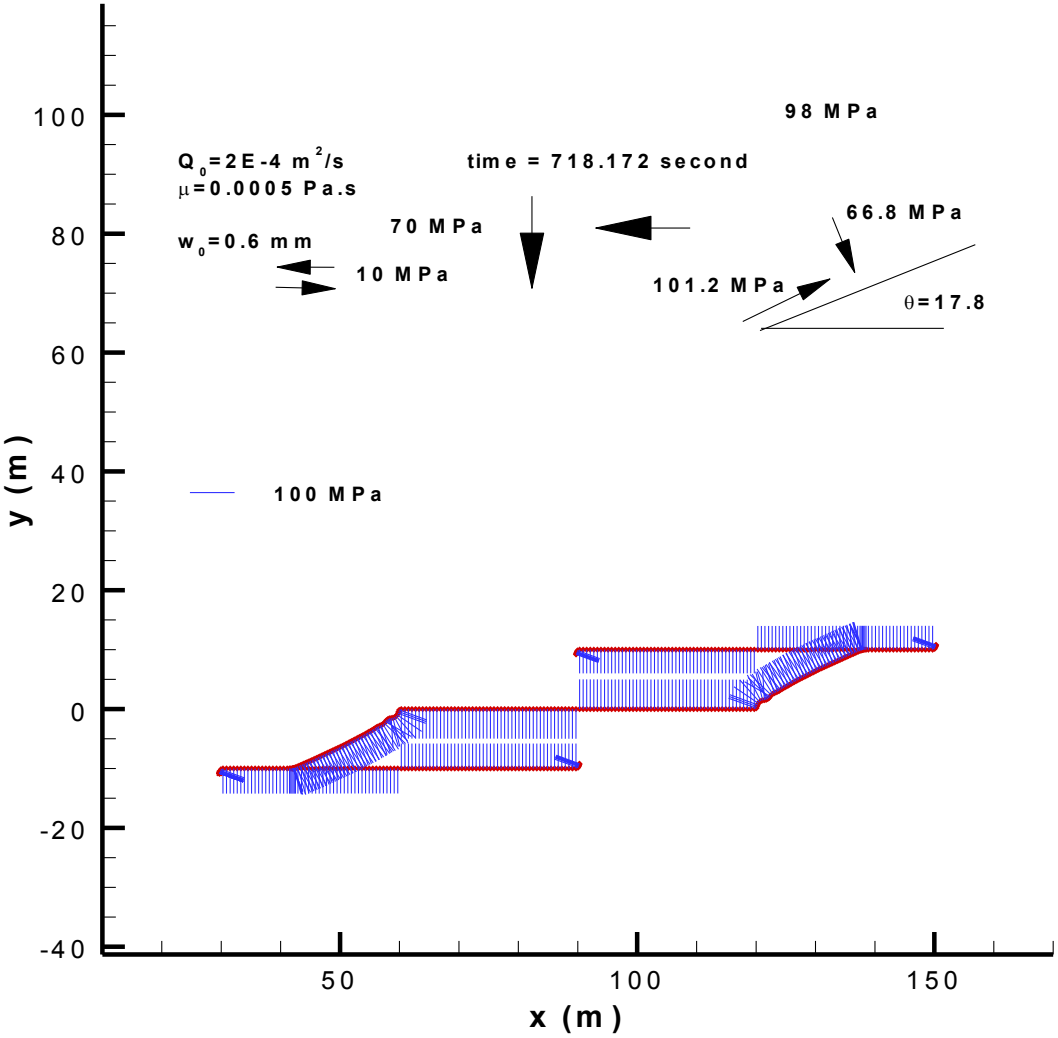

(c) Pressure (injection pressure is 66.6 MPa and the pressure drops rapidly near the intersection (to 59.2 MPa at 2 cm past the intersection)

Figure 10: (a) Fracture opening, (b) slip and (c) fluid pressure along the fractures at a specified time.

At the time shown, the pressure is very low along the upper and lower natural fracture, although the fluid has filled parts of them. The low pressure delays the development of shear on these fractures and wing fracture growth has not occurred from them. The cause of the low pressure fluid pressure lies in the narrow width of the wing fractures near the intersection point. In turn, this restriction results in higher pressure upstream of it which increases the width of the wing fracture segments making the connection. In contrast to the case shown in Figure 9, in this case the process of the wing fracture growth and the connection was calculated by the model, resulting in a connection with an acute angle which in turn leads to a strong interaction between the wing fracture and the natural fracture at this connecting point.

4 HYDRAULIC FRACTURE STIMULATION

Hydraulic fracture growth is driven by fluid injected at a rate sufficient to increase the pressure to a value exceeding the minimum principal stress magnitude, which in an unfractured rock mass results in fractures that grow with an orientation that is perpendicular to the minimum stress. In a fractured rock mass, the hydraulic fractures interact with the natural fractures and the fracture geometry becomes more complicated. The interactions can result in branching, blunting, or offsetting of the fracture (Warpinski and Teufel, 1987; Daneshy, 2003; Jeffrey et al., 2009a; Jeffrey et al., 2009b; Zhang and Jeffrey, 2006). Mineback mapping of hydraulic fractures placed into naturally fractured rock have revealed that the fracture path is planar overall but contains a number of branches and numerous offsets along this path. Figure 11 contains a photograph of a hydraulic fracture that was propped with green plastic proppant to mark its path. The fracture has developed a small offset where it interacted with and crossed a calcite-quartz vein (Jeffrey et al., 2009a; Jeffrey et al., 2010).

Figure 11: A photograph of a green-plastic propped hydraulic fracture crossing a calcite and quartz vein and leaving behind an offset. The scale is in millimeters and centimeters (after Jeffrey et al., 2009a).

The mineback experiment described in Jeffrey et al. (2009a) documented fractures consisting of a primary single propped channel with a number of offsets developing at natural fracture and vein crossing sites. Five hydraulic fractures were mapped at this site and all exhibited these general features. The fractures, which were formed by injection of 10 to 15 m^3 of water or crosslinked gel fluid at a rate of approximately 300 liters per minute, were found to extend to more than 20 m in half length. A composite map of the fractures is shown in Figure 12, with the grid shown at 20 m intervals for the northing and 10 m intervals for the easting. These findings are reinforced by mineback experiments at other sites, which also revealed similar offset fracture development in naturally fracture rock (Bunger et al., 2011; van As and Jeffrey, 2002). Thus, it is found that opening mode hydraulic fractures can be extended through naturally fractured rock and the process **does not** inevitably result in so much shear induced dilation that opening mode fractures cannot be extended.

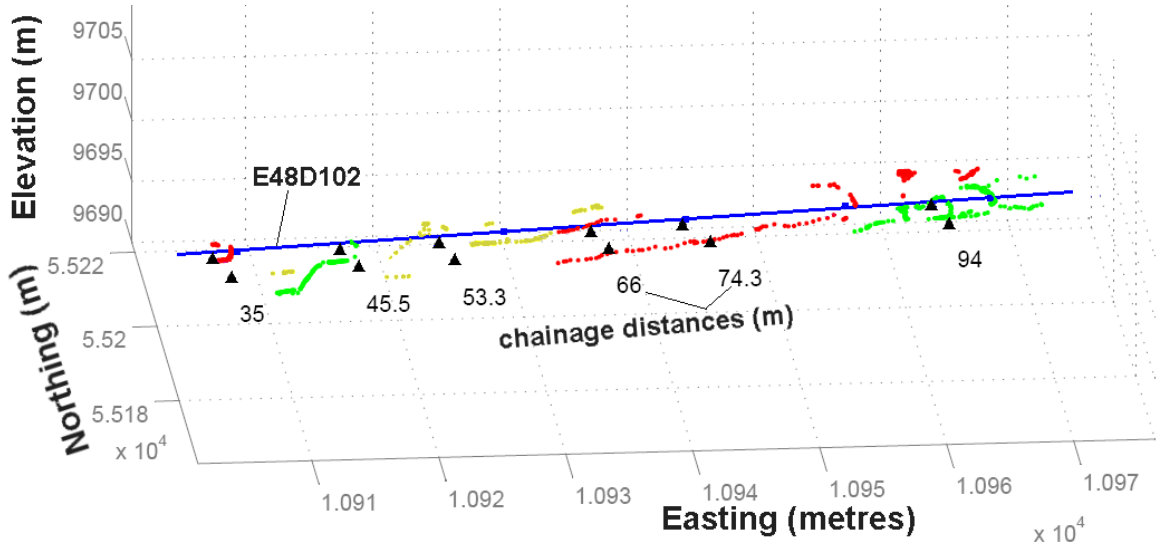

Figure 12: An oblique view showing the mapped extent of the five hydraulic fractures mined at the mineback experiment site. The fractures were mapped along both sides of a tunnel driven along the axis of the borehole (E48D102) from which the hydraulic fractures were place using a straddle packer system (after Jeffrey et al., 2009a).

An idealized fracture geometry (Figure 13) with offsets along its path has been used to numerically study the influence of these offsets on the fracture growth. The hydraulic fracture growth is guided along the path shown in Figure 13 by pre-meshing this path and not allowing any other paths to develop. The growth of such a fracture is affected strongly by the presence of the offsets. The offsets are locations of restricted opening of the hydraulic fracture, both because their orientation means they must open against a higher in situ normal stress and because they tend to be shorter in length and therefore are opened less at the same internal pressure compared with a longer fracture segment. The process of growth of a fracture along an offset path is illustrated in Figure 14 where a sequence of numerically calculated pressure and opening curves are given for progressively longer injection times.

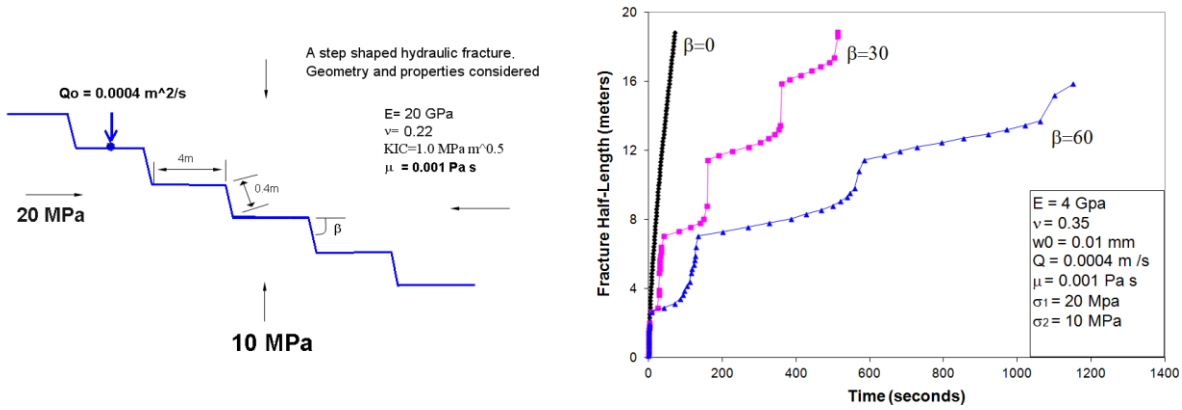

Figure 13: The fracture geometry is shown on the left side (the fracture is symmetric around the injection point with 4 offsets on each side although only part of the fracture is shown on the left of the injection point) and the growth (for a low value of Young's modulus) is shown on the right side as a function of the offset angle.

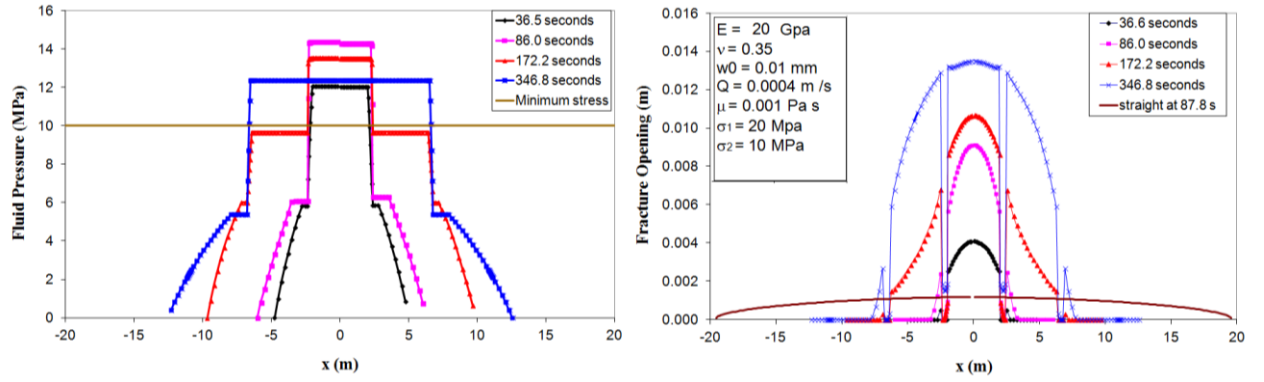

(a) (b)

Figure 14: The fracture pressure distribution (a) and opening distribution (b) for a 2D fracture with offsets as shown in Figure 13. A corresponding case for a straight fracture without offsets is also shown for comparison.

This fairly simple 2D model of growth through offsets reproduces responses that are associated with fracturing injections in naturally fracture rocks. Treatments in naturally fractured rock result in high net fracturing pressures and during the early parts of the treatment the injection pressure is often seen to increase for some time after fracture initiation. In Figure 14, the pressure is seen to increase with time until after 86 seconds and the net pressure at the well is 3 or 4 MPa whereas in a straight fracture this net pressure would be less than 0.5 MPa. The restricted opening at the offsets results in high viscous friction losses as the fluid is forced through them, with a high excess pressure in the fracture upstream of the offset, with this high pressure resulting in a wider fracture opening in the upstream portion. The wider fracture opening results in a slower fracture growth, as shown in the right side of Figure 13. For comparison, the opening and growth curve for a straight fracture without offsets is also shown in Figure 13 and Figure 14.

5 DISCUSSION AND CONCLUSIONS

The wing fracture growth mechanism can extend a linked system of natural fractures and wing fractures to considerable distance in a geothermal reservoir. The wide opening generated at the root of the wing fractures combined with shear-induced dilation along the fractures is likely to generate a conductive system of fractures for circulation of fluids through an EGS reservoir. Wing fractures tend to form and grow towards the maximum principal stress direction. The wing fracture linking mechanism would thus extend the fracture chain primarily horizontally into the reservoir in a thrust or strike slip fault stress environment, but vertically in a normal fault stress environment. A number of wing fracture chains could be formed from different isolated sections along the wellbore in the case where growth of the chain was in the horizontal direction. In a normal fault stress environment, two vertically separated horizontal wellbores might be used with a number of wing fractures chains grown to connect between them. In either case, the wing fracture and natural fracture chain will be oriented at a small angle to the maximum stress direction and the fracturing will be localized to a narrower zone. However, some shearing and dilation will always occur wherever fluid pressure can penetrate into the rock mass.

The 2D hydraulic fracture modeling of an opening mode fracture with offsets provides a simple model that is consistent with observed pressure and growth rate data from treatments in naturally fracture rock masses. However, the pressure, opening and growth predicted do not account for the 3D nature of the fractures being formed. The viscous fluid in a 3D fracture may partially bypass a restriction in the fracture plane caused by an offset. This bypassing would then reduce the net pressure because less flow would be forced through the narrower parts of the fracture channel. However, the general behavior seen in the 2D model are consistent with mineback data and with treating data from hydraulic fractures placed into naturally fractured reservoirs. A number of opening mode hydraulic fractures can be grown into a naturally fractured rock to form conductive connections between an injection and production well pair. Again, a method to treat individual isolated zones is required to allow this process to occur. These fractures will be self propping to some degree because of the shearing that occurs on them which is induced by shear mobilized on natural fractures that they cross and grow along for short distances (the offset portions). Additional proppant may or may not need to be placed in the fractures to increase the conductivity left after the injection stops.

The results presented here suggest that hydraulic fractures of considerable extent can be formed in EGS reservoir rock, provided only that a means of isolating sections of the well is available. Cemented casing followed by perforation to selectively gain connection to the reservoir is a proven method that would allow 10 to 20 or more zones to be stimulated using one of these methods.

A combined stimulation strategy may also prove to be useful where hydraulic fracturing is first carried out into a number of zones along a cased and cemented wellbore. During this phase of the operation, considerable shear induced conductivity will be generated as fluid from the fracturing operations leaks off into the rock surrounding the main hydraulic fracture plane. Additional shear stimulation with wing fracture growth can be used to extend the enhanced conductivity zone by later injection into the well with a limit on the injection pressure that maintains the pressure below the minimum principal stress magnitude.

REFERENCES

Bunger, A. P., R. G. Jeffrey, J. Kear, X. Zhang, M. Morgan: Experimental investigation of the interaction among closely spaced hydraulic fractures, *Proceedings* 45th US Rock Mechanics/Geomechanics Symposium, San Francisco, CA, June 26–29, (2011), 1-11.

Cooke, M. L.: Fracture localization along faults with spatially varying friction, *J. Geophys. Res.*, 102 (1997) 22425–22434.

Cotterell, B. and J. R. Rice: Slightly curved or kinked cracks, *Int. J. Fract.* 16 (1980), 155-169.

Daneshy, A. A.: Hydraulic Fracture Propagation in the Presence of Planes of Weakness. *Proceedings* SPE European Spring Meeting. Amsterdam, (1974) 1–5.

Daneshy, A.: Off-Balance Growth: A New Concept in Hydraulic Fracturing. *Journal of Petroleum Technology*, (April 2003), 78–85.

Detournay, E.: Propagation regime of fluid-driven fractures in impermeable rocks, *Int. J. Geomech*., 4, (2004) 35–45.

Dyskin A. V., L. N. Germanovich and K. B. Ustinov: A 3-D model of wing fracture growth and interaction, *Eng. Fract. Mech.* 63, (1999) 81-110.

Erdogan, E. and Sih G. C.: On the crack extension in plates under plane loading and transverse shear, *J. Basic Engineering* 85, 519-525 (1963).

Fairhurst, C. and N. G. W. Cook: The phenomenon of rock splitting parallel to the direction of maximum compression in the neighborhood of a surface. *Proceedings* First Congress International Society for Rocks Mechanics, Lisbon (1966).

Jeffrey, R., A. Bunger, B Lecampion, X Zhang, Z. Chen, A. van As, D. Allison, et al.: Measuring Hydraulic Fracture Growth in Naturally Fractured Rock. *Proceedings* SPE Annual Technical Conference and Exhibition, (2009a) 1–18.

Jeffrey, R., Zhang, X. and Bunger, A.: Hydraulic Fracturing of Naturally Fractured Reservoirs. *Proceedings* Thirty-Fifth Workshop on Geothermal Reservoir Engineering. Stanford University, Stanford, CA (2010), 1–9.

Jeffrey, R., Zhang, X. and Thiercelin, M.: Hydraulic Fracture Offsetting in Naturally Fractured Reservoirs: Quantifying a Long-Recognized Process. *Proceedings* SPE Hydraulic Fracturing Technology Conference. The Woodlands, TX (2009b).

Jung, R.: EGS – Goodbye or Back to the Future, *Proceedings* International Conference for Effective and Sustainable Hydraulic Fracturing, Brisbane (2013) Bunger, McLennan, and Jeffrey (editors) InTech. http://dx.doi.org/10.5772/56458

Kachanov, M. L.: A Microcrack model for rock inelasticity: Part I: Frictional sliding on mirocracks, *Mech. Mater*. 1 (1982) 19-27.

Lehner, F. and M. Kachanov: On modeling of "winged" cracks forming under compression, Int. J. Fract. 77, (1996) R69-R75.

Lockner, D. a., and J. D. Byerlee: Dilatancy in hydraulically isolated faults and the suppression of instability, *Geophysical Research Letter* 21, (1994), 2353-2356.

Multu, O. and D. D. Pollard: On the patterns of wing fractures along an outcrop scale flaw: A numerical modeling approach using complementarity, *J. Geophys. Res.* 113, B06403 (2008).

Namat-Nasser, S. and H. Horii: Compression-induced nonplanar crack extension with application to splitting, exfoliation and rockburst, *J. Geophys. Res.*, 87, (1982) 6805-6821.

Sahouryeh, E., A. V. Dyskin and L. N. Germanovich: Crack growth under biaxial compression, *Eng. Fract. Mech.* 69 (2002), 2187-2198.

Smith, M.C., Aamodt, R.L., Potter, R.M. and Brown, D.W. Manmade geothermal reservoirs, *Proceedings* 2nd US Symposium on Geothermal Energy, (1975) San Francisco, CA 1781-1787.

van As, A. and Jeffrey, R.: Hydraulic fracture growth in naturally fractured rock: mine through mapping and analysis. *Proceedings* NARMS-TAC (2002).

Verma, A., and Pruess, K.: Enhancement of Steam Phase Relative Permeability Due to Phase Transformation Effects in Porous Media, *Proceedings,* 11th Workshop on Geothermal Reservoir Engineering, Stanford University, Stanford, CA (1986).

Wang, C.T., and Horne, R.N.: Boiling Flow in a Horizontal Fracture, *Geothermics*, 29, (1999), 759-772.

Warpinski, N. and Teufel, L.: Influence of geologic discontinuities on hydraulic fracture propagation. *Journal of Petroleum Technology*, (February 1987). 209–220.

Weng, X., Kresse, O., Wu, R., and Guo, H.: Modeling of Hydraulic Fracture Network Propagation in a Naturally Fractured Formation. *Proceedings* SPE Hydraulic Fracturing Technology Conference. The Woodlands, TX (2011)

Zhang, X. and Jeffrey, R.G.: The role of friction and secondary flaws on deflection and re-initiation of hydraulic fractures at orthogonal pre-existing fractures. *Geophysical Journal International*, **166**, (2006) 1454–1465.

Zhang, X. and Jeffrey, R.G.: Reinitiation or termination of fluid-driven fractures at frictional bedding interfaces. *Journal of Geophysical Research*, **113**(B8), (2008) 1–16.

Zhang, X., R. G. Jeffrey, and M. Thiercelin: Deflection of fluid-driven fractures at bedding interfaces: A numerical investigation, *Journal of Structural. Geol*ogy, 29, (2007) 396–410.